Therapeutic potential of appropriately evaluated safe-induced pluripotent stem cells for spinal cord injury

Osahiko Tsuji[a,b,1], Kyoko Miura[a,c,1], Yohei Okada[a,d], Kanehiro Fujiyoshi[a,b], Masahiko Mukaino[a,e], Narihito Nagoshi[a,b,f], Kazuya Kitamura[a,b], Gentaro Kumagai[a,g], Makoto Nishino[a], Shuta Tomisato[a], Hisanobu Higashi[a], Toshihiro Nagai[h], Hiroyuki Katoh[a,b,f], Kazuhisa Kohda[a], Yumi Matsuzaki[a], Michisuke Yuzaki[a], Eiji Ikeda[i,j], Yoshiaki Toyama[b], Masaya Nakamura[b,2], Shinya Yamanaka[c], and Hideyuki Okano[a,2]

Departments of [a]Physiology and [b]Orthopedic Surgery, School of Medicine, Keio University, Shinjuku, Tokyo 160-8582, Japan; [c]Center for Induced Pluripotent Stem Cell Research and Application, Kyoto University, Kyoto 606-8507, Japan; [d]Kanrinmaru-Project and Departments of [e]Rehabilitation Medicine, [h]Electron Microscope Laboratory, and [i]Pathology, School of Medicine, Keio University, Tokyo 160-8582, Japan; [f]Department of Orthopedic Surgery, National Hospital Organization, Murayama Medical Center, Tokyo 208-0011, Japan; [g]Department of Orthopedic Surgery, Graduate School of Medicine, Hirosaki University, Aomori 036-8560, Japan; and [j]Department of Pathology, Graduate School of Medicine, Yamaguchi University, Yamaguchi 755-8505, Japan

Edited by Fred Gage, Salk Institute, San Diego, CA, and approved June 3, 2010 (received for review September 3, 2009)

Various types of induced pluripotent stem (iPS) cells have been established by different methods, and each type exhibits different biological properties. Before iPS cell-based clinical applications can be initiated, detailed evaluations of the cells, including their differentiation potentials and tumorigenic activities in different contexts, should be investigated to establish their safety and effectiveness for cell transplantation therapies. Here we show the directed neural differentiation of murine iPS cells and examine their therapeutic potential in a mouse spinal cord injury (SCI) model. "Safe" iPS-derived neurospheres, which had been pre-evaluated as nontumorigenic by their transplantation into nonobese diabetic/severe combined immunodeficiency (NOD/SCID) mouse brain, produced electrophysiologically functional neurons, astrocytes, and oligodendrocytes in vitro. Furthermore, when the safe iPS-derived neurospheres were transplanted into the spinal cord 9 d after contusive injury, they differentiated into all three neural lineages without forming teratomas or other tumors. They also participated in remyelination and induced the axonal regrowth of host 5HT$^+$ serotonergic fibers, promoting locomotor function recovery. However, the transplantation of iPS-derived neurospheres pre-evaluated as "unsafe" showed robust teratoma formation and sudden locomotor functional loss after functional recovery in the SCI model. These findings suggest that pre-evaluated safe iPS clone-derived neural stem/progenitor cells may be a promising cell source for transplantation therapy for SCI.

neural stem/progenitor cell | cell transplantation | regenerative medicine | remyelination | axonal regrowth

Given their ability to generate all types of neural cells, neural stem/progenitor cells (NS/PCs) are a promising source for cell replacement therapy for various intractable CNS disorders (reviewed in refs. 1–6). Notably, ES cells have great developmental plasticity and can be induced to become NS/PCs with specific differentiation potentials (7–11), making them a major candidate for cell replacement therapies for CNS disorders (12–16). The clinical use of ES cells is complicated, however, by ethical and immunological concerns, both of which might be overcome by using pluripotent stem cells derived directly from a patient's own somatic cells (17).

We recently reported the establishment of induced pluripotent stem (iPS) cells from mouse fibroblasts by the retroviral introduction of four factors (*Oct3/4*, *Sox2*, *Klf4*, and *c-Myc*) with selection for *Fbxo15* expression (18) and *Nanog* expression (19, 20). Compared with *Fbxo15*-selected iPS cells, *Nanog*-selected iPS cells more closely resembled ES cells' gene-expression pattern and could contribute to germline-competent adult chimeras (19–21). More recently, we and others (22, 23) generated iPS cells without using *c-Myc* retroviruses, albeit with lower efficiency. The successful establishment of these iPS cell lines, along with initial reports showing efficacy in the therapeutic use of iPS cells in rodent models of sickle cell anemia (24) and Parkinson disease (25), led us to examine the use of iPS cells as a treatment for spinal cord injury (SCI).

A number of important issues need to be addressed before a clinical trial using iPS cells as a cell-therapy source for SCI is initiated. First, a detailed evaluation of iPS cells' potential to generate neural cells compared with ES cells is required. Second, iPS cells are likely to carry a higher risk of tumorigenicity than ES cells, due to the inappropriate reprogramming of these somatic cells, the activation of exogenous transcription factors, or other reasons (25–27). Thus, it is essential to confirm the safety of grafted iPS-derived NS/PCs. Finally, the effectiveness of iPS-derived NS/PC transplantation as a treatment for SCI must be evaluated.

In the previous study, we pre-evaluated iPS clones for safety by transplanting iPS-derived neurospheres into the NOD/SCID mouse brain (27). Here, we show that the transplantation of neurospheres derived from safe iPS cell clones into the injured spinal cord promoted functional recovery without any tumor formation. In contrast, the transplantation of neurospheres derived from unsafe iPS cells, showing robust teratoma formation in the NOD/SCID mouse brain, also resulted in initial functional recovery, but was later followed by teratoma formation and deterioration of locomotor function. These data suggest that the evaluation of in vitro differentiation and in vivo tumorigenicity are important for identifying safe iPS clones for cell therapy, and that the NS/PCs derived from iPS clones deemed safe by such pre-evaluation are a promising source for cell therapy for SCI.

Results

Pre-Evaluated Safe MEF-iPS Cells Exhibit ES-Like Neural Differentiation Potentials in Vitro. We previously reported the neural differentiation of 36 independent murine iPS cell clones (27). The results of this study led us to classify several iPS clones as safe or unsafe

Author contributions: O.T., K.M., M. Nakamura, S.Y., and H.O. designed research; O.T., K.M., Y.O., K.F., M.M., N.N., K. Kitamura, G.K., M. Nishino, S.T., H.H., T.N., H.K., E.I., and H.O. performed research; O.T. and K.M. contributed new reagents/analytic tools; O.T., K.M., Y.O., K.F., M.M., N.N., K. Kitamura, G.K., H.K., K. Kohda, Y.M., M.Y., E.I., Y.T., M. Nakamura, S.Y., and H.O. analyzed data; and O.T., K.M., Y.O., K.F., H.K., E.I., M. Nakamura, and H.O. wrote the paper.

The authors declare no conflict of interest.

This article is a PNAS Direct Submission.

[1]O.T. and K.M. contributed equally to this work.

[2]To whom correspondence may be addressed. E-mail: hidokano@sc.itc.keio.ac.jp or masa@sc.itc.keio.ac.jp.

This article contains supporting information online at www.pnas.org/lookup/suppl/doi:10.1073/pnas.0910106107/-/DCSupplemental.

clones, according to the teratoma-forming activity of the iPS-derived neurospheres after transplantation into the NOD/SCID mouse brain.

Here, we first performed a detailed examination of the neural differentiation potential of a safe iPS clone, 38C2, which was established from mouse embryonic fibroblasts (MEFs) by the introduction of four factors, including *c-Myc*, and by the selection for *Nanog* expression (19, 28), and compared them with mouse ES cells (EB3) (29, 30). 38C2 iPS cells and EB3 ES cells were induced into embryoid bodies (EBs) in medium containing a low concentration of retinoic acid, then dissociated and cultured in suspension in serum-free medium with FGF-2 for 7 or 8 d to form primary neurospheres (PNS) (38C2 iPS/EB3 ES-PNS) (29). These PNSs were dissociated and formed secondary neurospheres (38C2 iPS/EB3 ES-SNS) under the same conditions (Fig. 1*A*). To induce further differentiation, 38C2 iPS-SNSs were adherently cultured in the absence of FGF-2, resulting in the generation of $Tuj1^+$ neurons ($4.9 \pm 0.8\%$), $GFAP^+$ astrocytes ($11.3 \pm 1.2\%$), and $CNPase^+$ oligodendrocytes ($3.7 \pm 0.9\%$), as well as $Nestin^+$ neural progenitor cells ($25.9 \pm 6.5\%$; Fig. 1 *B* and *C*), suggesting that 38C2 iPS-SNS have similar differentiation potentials to EB3 ES-SNS. The 38C2 iPS-PNSs could also generate TH^+ catecholaminergic, $5HT^+$ serotonergic, and $GAD67^+$ GABAergic neurons (Fig. S1). RT-PCR analysis of the expression of cell-type-specific markers in the progeny of the 38C2 iPS cells showed drastic decrease of the expression of undifferentiated ES cell marker genes, such as *Nanog*, *Eras*, and *Oct3/4*, and the up-regulation of neural markers such as *Sox1*, *βIII-tubulin,* and *GFAP* during the neural differentiation of 38C2 iPS cells, similar to EB3 ES cells (Fig. 1*D*).

Moreover, electrophysiological analysis using whole-cell patch clamping in both the 38C2 iPS-PNS– and EB ES-PNS–derived neurons after 21–28 d of adherent differentiation showed tetrodotoxin (TTX; 1 μM)-sensitive repetitive action potentials in the current-clamp mode [38C2 iPS-PNS (n = 11 of 16) and EB3 ES-PNS (n = 5 of 7)] (Fig. S2*A*) and very rapid inward currents immediately followed by transient outward currents in voltage-clamp mode (Fig. S2*B* 1 and 2). Steady outward currents, similar to those mediated by delayed-rectifier K^+ channels, were also observed (Fig. S2 *B*1 and *D*). These findings suggest that 38C2 iPS-PNSs produced neuronal cells equipped with functional channels that could generate and modify action potentials (*SI Text*).

Safe MEF-iPS Cells Can Differentiate into Trilineage Neural Cells in the Injured Spinal Cord Without Tumorigenesis. Previously, we confirmed that SNSs from the safe 38C2 MEF-iPS cell clone survived and showed no teratoma-forming activity in the NOD/SCID mouse brain for 24 wk after transplantation (27) (Fig. S3). 38C2 iPS-SNSs that were transplanted into the intact spinal cord survived and differentiated into trilineage neural cells without any tumorigenesis (Fig. S4). Next, to evaluate their therapeutic effects in the mouse SCI model, we transplanted 38C2 iPS-SNSs into the contused spinal cord 9 d after injury and compared them with EB3 ES-SNSs, using adult fibroblasts and PBS as controls. We also made a comparison with 38C2 iPS-PNSs, because we recently confirmed that the transplantation of ES cell-derived SNSs, but not PNSs, provides therapeutic benefit after SCI (31). We transplanted 38C2 iPS-SNSs that had been prelabeled by lentivirus to express both CBR*luc* and mRFP (32, 33) into the lesion epicenter 9 d after the injury. Bioluminescence imaging (BLI) analysis (34), which detects luciferase photon signals only from living cells, revealed an approximate graft survival rate of 18% at 35 d after transplantation (Fig. 2*A*). We also histologically confirmed that the grafted cells survived and exhibited no apparent evidence of tumorigenesis (Fig. 2*B*), and that there were no $Nanog^+$ cells (Fig. S5), at least during our observation

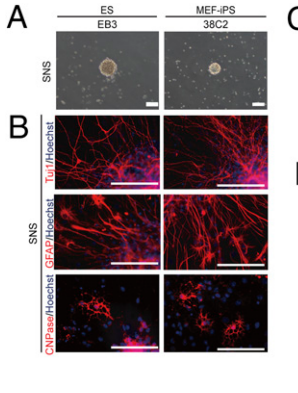

Fig. 1. Neural differentiation of pre-evaluated safe MEF-iPS cells in vitro. (*A*) Neurospheres derived from EB3 ES cells and 38C2 iPS cells. (Scale bar: 200 μm.) (*B*) Immunocytochemical analysis of neural cell marker proteins in the differentiated SNSs derived from EB3 ES and 38C2 iPS cells. (Scale bar: 100 μm.) (*C*) Neural differentiation efficiencies of neurospheres derived from EB3 ES and 38C2 iPS cells. (n = 5, n.s.). (*D*) RT-PCR analysis of undifferentiated cells (Un.), EBs, PNSs, SNSs, differentiated PNSs (PNS diff.), and SNSs (SNS diff.) of the EB3-ES and 38C2 iPS cells.

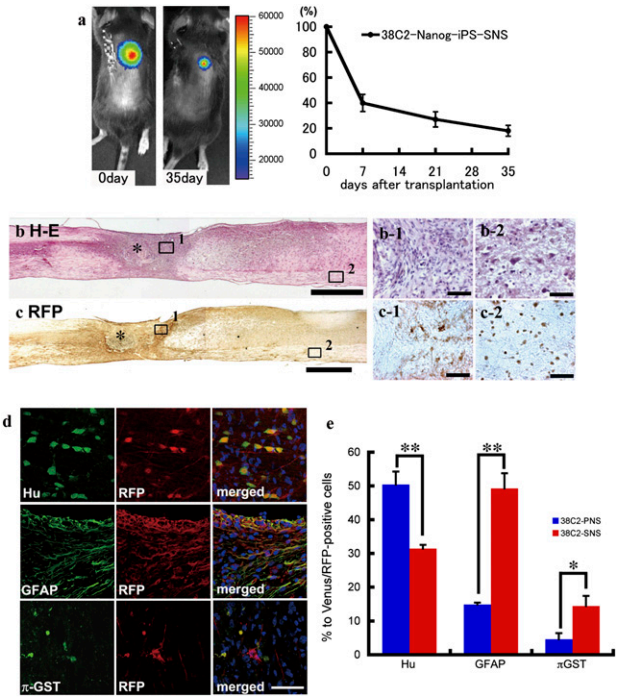

Fig. 2. Transplanted SNSs derived from safe MEF-iPS clones survive without any evidence of tumorigenesis and differentiate into trilineage neural cells in the injured spinal cord. (*A*) Representative BLI images of a mouse in which CBR*luc*-expressing 38C2 iPS-SNSs were transplanted into the injured spinal cord (*Left*, immediately after transplantation; *Right*, 42 d after transplantation). Quantification of the photon intensity revealed that ≈60% of the grafted cells were lost within 7 d after transplantation, and ≈20% of the cells survived 35 d after transplantation. Values are means ± SEM (n = 6). (*B*) H&E and (*C*) anti-RFP DAB staining of sagittal sections of the spinal cord 42 d after injury (38C2 iPS-SNS transplanted). There was no evidence of tumorigenesis (*B*). No significant nuclear atypia was observed in magnified images of the boxed areas showing the lesion epicenter (*B*-1) or white matter caudal to the transplantation site (*B*-2). Grafted cells survived and were diffusely distributed rostral and caudal to the lesion site (*C*). Higher-magnification images of the boxed areas showing the lesion site (*C*-1) and white matter caudal to the lesion site (*C*-2). *Lesion epicenter. (*D*) Immunohistochemical analyses of 38C2 iPS-SNSs grafted into spinal cord 42 d after injury, revealing grafted cells double-positive for RFP and markers of neural lineages. (*E*) Quantitative analyses of Hu^+ neurons, $GFAP^+$ astrocytes, and $\pi\text{-}GST^+$ oligodendrocytes. Values are means ± SEM (n = 3 each; $^*P < 0.05$, $^{**}P < 0.01$).

NEUROSCIENCE

period. Grafted RFP$^+$ cells were located mainly around the lesion epicenter, whereas some cells had migrated as far as 4 mm rostral and caudal to the graft site (Fig. 2*C*). In the injured spinal cord, the grafted 38C2 iPS-SNSs differentiated into three types of neural cells, including Hu$^+$ neurons (31.4 ± 1.1%), GFAP$^+$ astrocytes (49.3 ± 4.5%), and π-GST$^+$ oligodendrocytes (14.4 ± 3.0%), whereas 38C2 iPS-PNSs differentiated dominantly into neurons—that is, Hu$^+$ neurons (50.4 ± 3.8%), GFAP$^+$ astrocytes (14.9 ± 0.6%), and π-GST$^+$ oligodendrocytes (4.6 ± 1.8%) (Fig. 2 *D* and *E* and Fig. S6).

Transplantation of SNSs Derived from Safe MEF-iPS Cells into the Injured Spinal Cord Promotes Functional Recovery. The contusive SCI initially caused complete paralysis, followed by gradual recovery that reached a plateau. There were statistically significant differences in Basso mouse scale (BMS) between the 38C2 iPS-SNS and PBS groups at 21, 28, 35, and 42 d after injury, whereas no significant difference was observed between the 38C2 iPS-SNS and EB3 ES-SNS groups. Forty-two days after injury, the 38C2 iPS-SNS–grafted animals could lift their trunks and had significantly better BMS than the PBS control or adult fibroblast-treated animals, which were unable to support their body weight with their hindlimbs (Fig. 3*A*). To reveal the potential mechanism of functional recovery after 38C2 iPS-SNS transplantation, we conducted further histological analyses. By Luxol Fast Blue (LFB) staining, 38C2 iPS-SNS–grafted mice showed a significantly larger myelinated area at the lesion epicenter than the PBS control mice at 42 d after injury (Fig. 3*B*). We also found that grafted 38C2 iPS-SNS–derived cells myelinated NF200$^+$ host neuronal fibers, confirmed by the positive staining of RFP and myelin basic protein (MBP; Fig. 3*C*), indicating that graft cell-derived oligodendrocytes were capable of remyelination. For further confirmation of the myelinating ability of 38C2 iPS-SNSs, we transplanted 38C2 iPS-SNSs into the injured spinal cord of MBP-null *shiverer* mice, a severely hypo- and dysmyelinating mutant mouse that lacks the major dense line of CNS myelin (35). Myelinating potential of the grafted 38C2 iPS-SNS–derived cells was confirmed, exhibiting MBP$^+$ deposits (Fig. 3*D*) and the major dense line, by electron microscopic analysis (Fig. 3*E*).

To determine the effect of the grafted 38C2 iPS-SNSs on serotonergic nerve fibers, which are important for the motor functional recovery of hind limbs (36, 37), we immunostained for 5HT and quantified the positive area at the distal cord 1, 2, and 6 wk after injury. Some of the nerve fibers associated with graft cell-derived Hu$^+$ neurons were identified as 5HT$^+$ serotonergic fibers, and were prominent at the distal cord compared with the PBS control group (Fig. 4 *A*–*C*). Quantitative analysis of the serotonergic innervation of the distal cord revealed a significant difference between the 38C2 iPS-SNS and PBS control groups (Fig. 4*B*). The contusive injury (60 kDyn) resulted in a significant decrease in the number of 5HT$^+$ fibers at the distal cord, followed by a slight recovery, which is the nature of contusive SCI. The injection of PBS in the PBS control group did not induce any additional increase in the number of 5HT$^+$ fibers at the distal cord. In contrast, innervation of the distal cord by these 5HT$^+$ fibers was enhanced by the grafted 38C2 iPS-SNS 6 wk after SCI (Fig. 4*B*). Moreover, 38C2 iPS-SNS–derived astrocytes, which exhibited a bipolar morphology with long processes, were observed closely associated with the 5HT$^+$ serotonergic fibers (Fig. 4*D*).

Transplantation of Neurospheres Derived from Pre-Evaluated Safe or Unsafe TTF-iPS Cells into the Injured Spinal Cord. Toward the goal of clinical application, we next examined the therapeutic potential

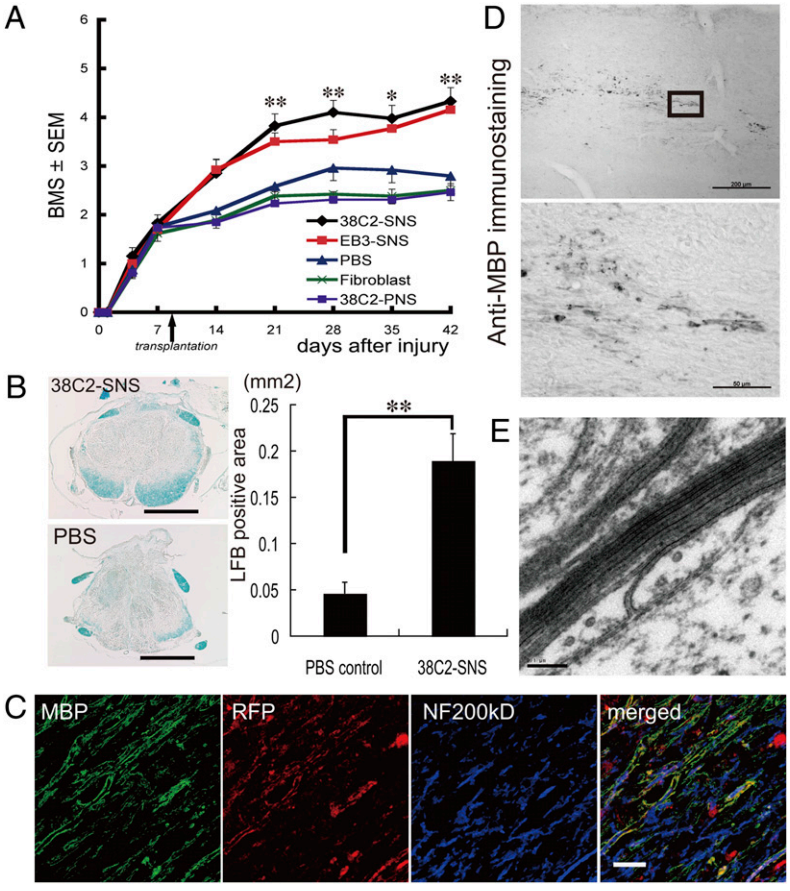

Fig. 3. SNS derived from a safe MEF-iPS clone differentiate into mature oligodendrocytes and promote remyelination. (*A*) Time course of functional recovery of hind limbs evaluated by BMS. 38C2 iPS-SNS, $n = 19$; EB3 ES-SNS, $n = 15$; PBS, $n = 12$; adult fibroblasts, $n = 13$; 38C2 iPS-PNS, $n = 13$. $^*P < 0.05$, $^{**}P < 0.01$. (*B*) LFB staining of axial sections of the spinal cord at the lesion epicenter 42 d after injury; 38C2 iPS-SNS–transplanted (*Upper Left*) and PBS control (*Lower Left*) animals. Quantification of LFB-positive areas at the lesion epicenter 42 d after injury (*Right*, $n = 7$ each; $^{**}P < 0.01$). (*C*) Immunohistochemistry of 38C2 iPS-SNS–derived mature oligodendrocytes (MBP$^+$). Grafted cells were integrated into myelin sheath. (*D*) Anti-MBP DAB staining of sagittally sectioned spinal cord of a *shiverer* mouse 8 wk after transplantation. MBP$^+$ myelin was detected in the area caudal to the lesion epicenter. (*Lower*) Higher-magnification image of the boxed area. (*E*) EM pictures of the injured spinal cord of a 38C2 iPS-SNS–grafted *shiverer* mouse exhibiting a prominent major dense line and intraperiod lines in multiple compacted lamellae. (Scale bars: *B*, 500 μm; *D Upper*, 200 μm; *C* and *D Lower*, 50 μm; and *E*, 0.1 μm.)

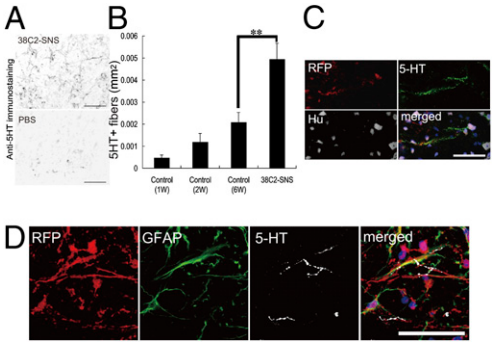

Fig. 4. SNSs derived from a safe MEF-iPS clone promote serotonergic innervation of the dorsal cord and result in better functional recovery of the hindlimbs. (*A*) 38C2 iPS-SNS transplantation promoted the growth of 5HT$^+$ serotonergic fibers in the distal spinal cord. Axial sections of 38C2 iPS-SNS–transplanted (*Upper*) and PBS control mice (*Lower*). (*B*) Quantitative analysis of 5HT$^+$ serotonergic fibers of distal cord in the PBS control (1, 2, and 6 wk postinjury) and 38C2 iPS-SNS transplantation groups (6 wk postinjury; 1 and 2 wk postinjury, $n = 3$ each; 6 wk postinjury and 38C2 SNS, $n = 7$ each; $^{**}P < 0.01$). (*C* and *D*) Immunohistochemistry of 38C2 iPS-SNS–derived neurons (*C*, RFP$^+$, Hu$^+$) and astrocytes (*D*, RFP$^+$, GFAP$^+$) closely associated with 5HT$^+$ serotonergic fibers. (Scale bars: *A*, 100 μm; *C*, 20 μm; *D*, 50 μm.)

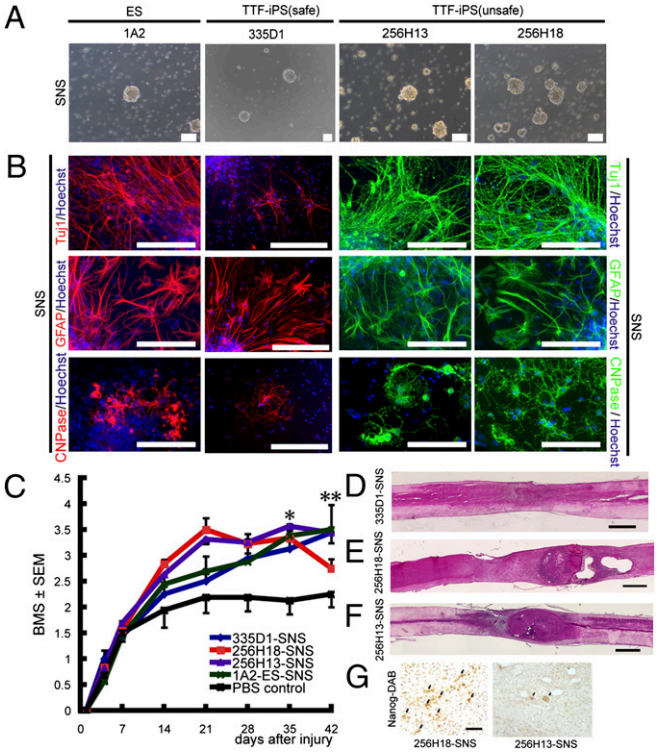

Fig. 5. Characterization and transplantation of SNSs derived from safe and unsafe TTF-iPS cells. (*A*) Neurospheres derived from 1A2 ES cells, 335D1, 256H13, and 256H18 iPS cells. (Scale bar: 200 μm.) (*B*) The differentiation potential of TTF-iPS-derived SNSs tested in vitro by immunocytochemical analyses of neural cell markers; Tuj1 for neurons, GFAP for astrocytes, and CNPase for oligodendrocytes. (Scale bar: 100 μm.) (*C*) Time course of functional recovery of the hindlimbs evaluated by BMS. 335D1 iPS-SNS: $n = 9$ each; 256H13 and 256H18 iPS-SNS: $n = 9$; 1A2 ES-SNS: $n = 9$; PBS control: $n = 8$. $^*P < 0.05$, $^{**}P < 0.01$. (*D*–*F*) H&E sagittal sections of the spinal cord 42 d after injury. (*D*) 335D1 iPS-SNS, (*E*) 256H18 iPS-SNS, and (*F*) 256H13 iPS-SNS grafted mice. There was no evidence of tumorigenesis in the 335D1 iPS-SNS grafted mice (*D*), whereas teratoma formation was detected within the injured spinal cord in both 256H18 iPS-SNS (*E*), and 256H13 iPS-SNS (*F*) grafted mice. (*G*) Anti-Nanog DAB staining of sagittally sectioned spinal cord of 256H18 and 256H13 iPS-SNS–transplanted animals 35 d after transplantation.

of adult tissue-derived iPS cells. Among six TTF-iPS clones pre-evaluated in our previous study (27), we used the safe 335D1 TTF-iPS clone, which was generated with *Nanog* selection and without the transduction of c-Myc. We also used the unsafe 256H13 and 256H18 TTF-iPS clones (22, 27), which were generated without genetic selection or the transduction of c-Myc, and were originally established from CAG-EGFP mice (22). A subclone of RF8 ES cells carrying the *Nanog*-EGFP reporter (1A2) (19) was used as control. All of the TTF-iPS clones formed PNSs and SNSs (Fig. 5*A*), and generated cells of all three neural lineages, similar to those derived from 1A2 ES cells (Fig. 5*B*). We transplanted these TTF-iPS–derived SNSs into injured spinal cords 9 d after injury. Transplantation of the safe 335D1 iPS-SNS (prelabeled with RFP lentivirally) resulted in better functional recovery compared with the PBS control group, without any apparent tumorigenesis during our observation period (Fig. 5 *C* and *D*). Grafted and survived RFP$^+$ 335D1 iPS-SNS–derived cells could differentiate into neural trilineages (Fig. S7 *A* and *B*). Furthermore, LFB staining revealed that 335D1 iPS-SNS–grafted mice had a significantly larger myelinated area at the lesion epicenter than the PBS control mice at 42 d after injury (Fig. S8 *A* and *B*), and grafted RFP$^+$ 335D1 SNS-derived cells differentiated into MBP$^+$ oligodendrocytes (Fig. S8*C*). However, all unsafe 256H18 iPS-SNS–grafted mice and one of 256H13 iPS-SNS–grafted mice formed teratomas containing EGFP$^+$ donor cells within the injured spinal cord (Fig. 5 *E* and *F* and Fig. S7*C*). Histological analyses revealed that these teratomas contained epithelial and smooth muscle tissue (Fig. S9*A*), and also exhibited Nanog immunoreactivity (Fig. 5*G*). Although the motor functions gradually recovered in both groups to the same extent as in the safe 335D1 iPS-SNS recipients until 35 d after injury, the 256H18 iPS-SNS–grafted animals exhibited a sudden deterioration of motor function 42 d after injury. In contrast, the 256H13 iPS-SNS–grafted animals maintained their functional recovery at 42 d after injury (Fig. 5*C*). Notably, in most mice of the 256H13 iPS-SNS group, scattered small clusters of Nanog$^+$ cells were observed in the spinal cords without obvious teratoma formation (Fig. S9 *B* and *C*). Thus, we speculate that teratoma formation and subsequent deterioration of function recovery would occur in the 256H13 group if a longer observation period was set.

Discussion

In the present study, we showed that the pre-evaluated safe iPS cells could produce neurospheres containing NS/PCs (Fig. 1*A*) that give rise to trilineage neural cells, including several types of neurons (Fig. 1 *B* and *C*), and that the neurons were electrophysiologically functional in vitro similar to ES cells (Fig. S2).

Based on these safety assessments and in vitro findings, we performed an in vivo study using the safe 38C2 MEF-iPS cell clone. Grafted 38C2 iPS-SNSs differentiated into neurons, astrocytes, and oligodendrocytes without forming teratomas or other tumors, and promoted functional recovery after SCI, whereas 38C2 iPS-PNSs did not show any therapeutic effects (Fig. 3*A*). These findings were compatible with our recent data on mouse ES cell-derived neurosphere transplantation into an identical mouse SCI model (31). Transplantation of ES-derived SNSs, which can differentiate into neural trilineages, promoted remyelination, axonal regrowth and tissue sparing, leading to improved function. In contrast, predominantly neurogenic PNSs showed no therapeutic effects on SCI (31). Thus, we elected to use iPS-SNSs and not iPS-PNSs for this study. In fact, the grafted 38C2 iPS-SNSs formed MBP$^+$ myelin sheaths within the injured spinal cord. We also confirmed the myelination potential of 38C2 iPS-SNS–derived cells in the spinal cord of the MBP-null *shiverer* mouse by electron microscopy (Fig. 3

D and *E*). These findings suggested the possibility of the remyelination of demyelinated axons by the grafted 38C2 iPS-SNS–derived oligodendrocytes, which may have contributed to the functional recovery of the grafted animals.

Another potential mechanism for functional recovery is axonal regrowth supported by iPS-SNS–derived astrocytes. Here, we observed grafted 38C2 iPS-SNS–derived $GFAP^+$ astrocytes, which exhibited a bipolar morphology with long processes extending along the axis of the spinal cord, caudal to the lesion epicenter, in close association with $5HT^+$ host serotonergic fibers (Fig. 4*D*). A previous report indicated that immature astrocytes derived from cells grafted into the injured spinal cord promote the outgrowth of $5HT^+$ fibers by offering a growth-permissive surface (38). Consistent with this finding, the transplantation of 38C2 iPS-SNSs promoted serotonergic innervation of the distal cord compared with the PBS control animals, thereby enhancing functional recovery after SCI (Fig. 4 *A* and *B*) (36). Furthermore, trophic factors, such as neurotrophin-3 (NT-3) and brain-derived neurotrophic factor (BDNF), were expressed in 38C2 iPS-SNSs, which could act as an integral part of the observed functional recovery (39, 40). The tissue sparing (e.g., neuroprotection, axon sprouting and remyelination) and other effects, including functional remodeling of spinal locomotor circuits (41), of trophic factors secreted from grafted cells are considered to be important for functional recovery (42). Thus, the combined effects of the 38C2 iPS-SNS–derived glial cells probably contributed to locomotor function recovery.

For clinical applications, the findings with TTF-iPS cells were promising, as most SCI patients are adults. The transplantation of SNSs derived from a pre-evaluated safe TTF-iPS clone promoted functional recovery after SCI without teratoma formation, like the SNSs from safe MEF-iPS clone did (Fig. 5*D*). However, the transplantation of SNSs derived from the unsafe TTF-iPS cells resulted in teratoma formation and functional deterioration. The teratoma-forming activity of TTF-iPS-SNSs could be caused by the presence of undifferentiated cells that might be resistant to differentiation signals within the SNSs (27). In fact, we recently reported that persistent presence of undifferentiated cells within iPS-SNSs highly correlated with teratoma-forming propensity, assayed by flow cytometric analysis using *Nanog*-EGFP reporter and transplantation into the brains of immunodeficient (NOD/SCID) (27). Before iPS cells of adult origin can be used clinically, important hurdles must still be overcome. Though new methods for establishing iPS cells are constantly being developed, including virus-free (43) and transgene-free (44) systems, a new strategy is needed to exclude undifferentiated cells from the differentiated progeny of iPS cells. These findings show that the pre-evaluation of iPS cells' in vitro differentiation potential could play a critical role in terms of their safety and therapeutic effects on the mouse SCI model. Thus, iPS-derived neurosphere transplantation has potential therapeutic use in SCI, when the iPS cell clones are carefully pre-evaluated.

From a clinical viewpoint, it is particularly encouraging that delaying the iPS-derived NS/PC transplantation (to 9 d after injury) enhanced both the survival of the grafted cells and functional recovery, the therapeutic effects of which is almost comparable to those of fetal CNS-derived NS/PCs transplantation (refs. 34 and 45). This finding may also be applicable to the treatment of patients with SCI. Since our first report of iPS cells (18), there has been increasing interest in their characteristics and therapeutic potential. Our present study demonstrates the therapeutic potential of iPS-derived NS/PCs for SCI repair. Before any clinical trial of human CNS disorders using iPS cells, it will be essential to pre-evaluate each iPS cell clone carefully to guarantee a safety level equal to other types of cells, such as Schwann cells (46, 47) and fetal-derived neurosphere cells (NS/PCs) (3), and to conduct preclinical transplantation studies using appropriate primate models (48, 49).

Methods

Reverse-Transcription and RT-PCR. RNA was isolated with TRIzol (Invitrogen) according to the manufacturer's instructions. Total RNA (0.5 μg) was treated with TURBO DNase (Ambion) and then reverse-transcribed with oligo (dT) primer and SuperScript III (Invitrogen). The primers and PCR conditions used in this study are listed Table S1.

Cell Culture, Neural Induction, and Immunocytochemistry. Mouse ES and iPS cells were cultured as described previously (19, 28, 29). Mouse ES and iPS cells were differentiated into neurospheres via EBs treated with 10^{-8} M retinoic acid (Sigma), as described previously with minor modification (28, 29). (Detailed differentiation protocol is described in *SI Text*.) ES and iPS cell-derived neurospheres were dissociated and differentiated on poly-L-ornithine/fibronectin-coated coverslips for 5 d and subjected to immunocytochemical analysis. The number of cells immunoreactive for each marker was counted and shown as the percentage of the total number of cells counterstained with Hoechst 33258. The antibodies used in this study are listed in Table S2.

Lentivirus Production and Infection of Secondary Neurospheres. For BLI tracing of grafted 38C2 iPS-SNSs, we generated a modified lentivirus vector encoding both the click beetle red luciferase (CBR/*uc*; Promega) and mRFP, pCSII-EF-CBR/*uc*-IRES2-mRFP (32, 33). For lentivirus preparation, HEK-293T cells were transfected with pCSII-EF-CBR/*uc*-IRES2-mRFP, pCAG-HIVgp, and pCMV-VSV-G-RSV-Rev, and the conditioned medium containing virus particles was concentrated and used for viral transduction.

Spinal Cord Injury Model and Transplantation. Adult female C57BL/6J mice (20–22 g) were anesthetized via an i.p. injection of ketamine (100 mg/kg) and xylazine (10 mg/kg). A contusive spinal cord injury using an Infinite Horizon Impactor (60 kdyn; Precision Systems) was induced at the Th10 level as reported previously (34). For transplantation, 5×10^5 cells of mouse ES/iPS cell-derived neurospheres, adult dermal fibroblasts in 2 μL of cell suspension, or PBS was injected into the lesion epicenter. Hindlimb motor function was evaluated by the locomotor rating of the Basso mouse scale (BMS) (50) for 42 d after injury. For the in vivo imaging of intact and injured spinal cords after the transplantation, a Xenogen-IVIS 100 cooled CCD optical macroscopic imaging system (SC BioScience) was used for BLI, as reported previously (34) (*SI Text*). All procedures were approved by the ethics committee of Keio University, and were in accordance with the Guide for the Care and Use of Laboratory Animals (National Institutes of Health). Grafted animals were deeply anesthetized and intracardially perfused with 4% paraformaldehyde (PFA; pH 7.4). The dissected spinal cords were sectioned into 20-μm axial/sagittal sections using a cryostat and processed for histological analyses. Detailed conditions for histological analyses are described in *SI Text*.

Statistical Analysis. All data are reported as the mean ± SEM. An unpaired two-tailed Student's *t* test was used for the analyses of in vitro and in vivo 38C2 iPS-SNS and ES-SNS differentiation efficiency (Figs. 1*C* and 2*E*), $5HT^+$ areas (Fig. 4*B*), and LFB^+ areas (Fig. 2*B*). Repeated-measures two-way ANOVA, followed by the Tukey–Kramer test, was used for BMS analysis. $^*P < 0.05$, $^{**}P < 0.01$.

ACKNOWLEDGMENTS. We thank Drs. H. Abe, T. Sunabori, F. Renault-Mihara, W. Akamatsu, S. Shibata, T. Harada, S. Miyao, and H. J. Okano (Keio University) for technical assistance and scientific discussions, and all the members of Dr. Okano's and Dr. Yamanaka's laboratories for encouragement and generous support. We also thank Drs. K. Okita, M. Koyanagi, and K. Tanabe (Kyoto University) for the undifferentiated iPS cells, Dr. H. Niwa (Riken CDB) for the EB3 ES cells, Dr. R. Farese (University of California-San Francisco) for the RF8 ES cells, Dr. R. Y. Tsien (University of California-San Diego) for the mRFP gene, Dr. A. Miyawaki (Riken BSI) for the Venus gene, Dr. H. Baba (Tokyo University of Phamacy and Life Science) for the shiverer mice, and Dr. H. Miyoshi (Riken BRC) for the lentiviral vectors. We especially thank Drs. S. Okada (Kyusyu University), A. Iwanami (University of California-San Francisco and Keio University), and J. Yamane (Keio University) for scientific discussions, technical advice, and encouragement. This work was supported by grants from the Program for Promotion of Fundamental Studies in Health Sciences of the National Institute of Biomedical Innovation (NIBIO), a grant from Uehara Memorial Foundation, and Grants-in-Aid for Scientific Research from the Japan Society for the Promotion of Science (JSPS) and the Ministry of Education, Culture, Sports, Science and Technology of Japan (MEXT), the project for realization of regenerative medicine and support for the core institutes for iPS cell research from MEXT; Japan Science and Technology Agency (SORST); the Ministry of Health, Labor, and Welfare; the General Insurance Association of Japan; Research Fellowships for Young Scientists from the Japan Society for the Promotion of Science; Keio Gijuku Academic Development Funds; and a Grant-in-aid for the Global COE program from MEXT to Keio University.

1. Björklund A, Lindvall O (2000) Cell replacement therapies for central nervous system disorders. *Nat Neurosci* 3:537–544.
2. Okano H (2002) Stem cell biology of the central nervous system. *J Neurosci Res* 69: 698–707.
3. Lindvall O, Kokaia Z, Martinez-Serrano A (2004) Stem cell therapy for human neurodegenerative disorders—how to make it work. *Nat Med* 10 (Suppl):S42–S50.
4. Martino G, Pluchino S (2006) The therapeutic potential of neural stem cells. *Nat Rev Neurosci* 7:395–406.
5. Lindvall O, Kokaia Z (2006) Stem cells for the treatment of neurological disorders. *Nature* 441:1094–1096.
6. Gage FH (2000) Mammalian neural stem cells. *Science* 287:1433–1438.
7. Wichterle H, Lieberam I, Porter JA, Jessell TM (2002) Directed differentiation of embryonic stem cells into motor neurons. *Cell* 110:385–397.
8. Watanabe K, et al. (2005) Directed differentiation of telencephalic precursors from embryonic stem cells. *Nat Neurosci* 8:288–296.
9. Sonntag KC, et al. (2007) Enhanced yield of neuroepithelial precursors and midbrain-like dopaminergic neurons from human embryonic stem cells using the bone morphogenic protein antagonist noggin. *Stem Cells* 25:411–418.
10. Tropepe V, et al. (2001) Direct neural fate specification from embryonic stem cells: A primitive mammalian neural stem cell stage acquired through a default mechanism. *Neuron* 30:65–78.
11. Ying QL, Stavridis M, Griffiths D, Li M, Smith A (2003) Conversion of embryonic stem cells into neuroectodermal precursors in adherent monoculture. *Nat Biotechnol* 21: 183–186.
12. McDonald JW, et al. (1999) Transplanted embryonic stem cells survive, differentiate and promote recovery in injured rat spinal cord. *Nat Med* 5:1410–1412.
13. Brüstle O, et al. (1999) Embryonic stem cell-derived glial precursors: A source of myelinating transplants. *Science* 285:754–756.
14. Kim JH, et al. (2002) Dopamine neurons derived from embryonic stem cells function in an animal model of Parkinson's disease. *Nature* 418:50–56.
15. Sharp J, Keirstead HS (2007) Therapeutic applications of oligodendrocyte precursors derived from human embryonic stem cells. *Curr Opin Biotechnol* 18:434–440.
16. Keirstead HS, et al. (2005) Human embryonic stem cell-derived oligodendrocyte progenitor cell transplants remyelinate and restore locomotion after spinal cord injury. *J Neurosci* 25:4694–4705.
17. Hochedlinger K, Jaenisch R (2006) Nuclear reprogramming and pluripotency. *Nature* 441:1061–1067.
18. Takahashi K, Yamanaka S (2006) Induction of pluripotent stem cells from mouse embryonic and adult fibroblast cultures by defined factors. *Cell* 126:663–676.
19. Okita K, Ichisaka T, Yamanaka S (2007) Generation of germline-competent induced pluripotent stem cells. *Nature* 448:313–317.
20. Wernig M, et al. (2007) In vitro reprogramming of fibroblasts into a pluripotent ES-cell-like state. *Nature* 448:318–324.
21. Maherali N, et al. (2007) Directly reprogrammed fibroblasts show global epigenetic remodeling and widespread tissue contribution. *Cell Stem Cell* 1:55–70.
22. Nakagawa M, et al. (2008) Generation of induced pluripotent stem cells without Myc from mouse and human fibroblasts. *Nat Biotechnol* 26:101–106.
23. Wernig M, Meissner A, Cassady JP, Jaenisch R (2008) c-Myc is dispensable for direct reprogramming of mouse fibroblasts. *Cell Stem Cell* 2:10–12.
24. Hanna J, et al. (2007) Treatment of sickle cell anemia mouse model with iPS cells generated from autologous skin. *Science* 318:1920–1923.
25. Wernig M, et al. (2008) Neurons derived from reprogrammed fibroblasts functionally integrate into the fetal brain and improve symptoms of rats with Parkinson's disease. *Proc Natl Acad Sci USA* 105:5856–5861.
26. Yamanaka S (2007) Strategies and new developments in the generation of patient-specific pluripotent stem cells. *Cell Stem Cell* 1:39–49.
27. Miura K, et al. (2009) Variation in the safety of induced pluripotent stem cell lines. *Nat Biotechnol* 27:743–745.
28. Okada Y, et al. (2008) Spatiotemporal recapitulation of central nervous system development by murine embryonic stem cell-derived neural stem/progenitor cells. *Stem Cells* 26:3086–3098.
29. Okada Y, Shimazaki T, Sobue G, Okano H (2004) Retinoic-acid-concentration-dependent acquisition of neural cell identity during in vitro differentiation of mouse embryonic stem cells. *Dev Biol* 275:124–142.
30. Niwa H, Miyazaki J, Smith AG (2000) Quantitative expression of Oct-3/4 defines differentiation, dedifferentiation or self-renewal of ES cells. *Nat Genet* 24:372–376.
31. Kumagai G, et al. (2009) Roles of ES cell-derived gliogenic neural stem/progenitor cells in functional recovery after spinal cord injury. *PLoS ONE* 4:e7706.
32. Masuda H, et al. (2007) Noninvasive and real-time assessment of reconstructed functional human endometrium in NOD/SCID/gamma c(null) immunodeficient mice. *Proc Natl Acad Sci USA* 104:1925–1930.
33. Miyoshi H, Blömer U, Takahashi M, Gage FH, Verma IM (1998) Development of a self-inactivating lentivirus vector. *J Virol* 72:8150–8157.
34. Okada S, et al. (2005) In vivo imaging of engrafted neural stem cells: Its application in evaluating the optimal timing of transplantation for spinal cord injury. *FASEB J* 19: 1839–1841.
35. Inoue Y, et al. (1986) Alteration of the primary pattern of central myelin in a chimaeric environment—study of shiverer ↔ wild-type chimaeras. *Brain Res* 391:239–247.
36. Bregman BS, et al. (1993) Recovery of function after spinal cord injury: Mechanisms underlying transplant-mediated recovery of function differ after spinal cord injury in newborn and adult rats. *Exp Neurol* 123:3–16.
37. Nygren LG, Fuxe K, Jonsson G, Olson L (1974) Functional regeneration of 5-hydroxytryptamine nerve terminals in the rat spinal cord following 5, 6-dihydroxytryptamine induced degeneration. *Brain Res* 78:377–394.
38. Hofstetter CP, et al. (2002) Marrow stromal cells form guiding strands in the injured spinal cord and promote recovery. *Proc Natl Acad Sci USA* 99:2199–2204.
39. Widenfalk J, Lundströmer K, Jubran M, Brene S, Olson L (2001) Neurotrophic factors and receptors in the immature and adult spinal cord after mechanical injury or kainic acid. *J Neurosci* 21:3457–3475.
40. McTigue DM, Horner PJ, Stokes BT, Gage FH (1998) Neurotrophin-3 and brain-derived neurotrophic factor induce oligodendrocyte proliferation and myelination of regenerating axons in the contused adult rat spinal cord. *J Neurosci* 18:5354–5365.
41. Courtine G, et al. (2009) Transformation of nonfunctional spinal circuits into functional states after the loss of brain input. *Nat Neurosci* 12:1333–1342.
42. Lu P, Tuszynski MH (2008) Growth factors and combinatorial therapies for CNS regeneration. *Exp Neurol* 209:313–320.
43. Okita K, Nakagawa M, Hyenjong H, Ichisaka T, Yamanaka S (2008) Generation of mouse induced pluripotent stem cells without viral vectors. *Science* 322:949–953.
44. Zhou H, et al. (2009) Generation of induced pluripotent stem cells using recombinant proteins. *Cell Stem Cell* 4:381–384.
45. Ogawa Y, et al. (2002) Transplantation of in vitro-expanded fetal neural progenitor cells results in neurogenesis and functional recovery after spinal cord contusion injury in adult rats. *J Neurosci Res* 69:925–933.
46. Pearse DD, et al. (2004) cAMP and Schwann cells promote axonal growth and functional recovery after spinal cord injury. *Nat Med* 10:610–616.
47. Pearse DD, et al. (2007) Transplantation of Schwann cells and/or olfactory ensheathing glia into the contused spinal cord: Survival, migration, axon association, and functional recovery. *Glia* 55:976–1000.
48. Iwanami A, et al. (2005) Establishment of graded spinal cord injury model in a nonhuman primate: The common marmoset. *J Neurosci Res* 80:172–181.
49. Iwanami A, et al. (2005) Transplantation of human neural stem cells for spinal cord injury in primates. *J Neurosci Res* 80:182–190.
50. Basso DM, et al. (2006) Basso Mouse Scale for locomotion detects differences in recovery after spinal cord injury in five common mouse strains. *J Neurotrauma* 23:635–659.